INL/RPT-23-73511

Research internship report

May, 1st 2023 - August, 18th 2023

Thermal Hydraulic Modeling of an Advanced Nuclear Reactor using open-source MOOSE tools

Sixte de Boisset[1,2] and Lise Charlot (Mentor)[2]

[1] *Idaho National Laboratory*
[2] *Ecole Polytechnique de Paris (Promotion X2020)*

INL is a U.S. Department of Energy National Laboratory
operated by Battelle Energy Alliance, LLC

INL/RPT-23-73511

Research internship report

Thermal Hydraulic Modeling of an Advanced Nuclear Reactor using open-source MOOSE tools

Sixte de Boisset[1,2] **and Lise Charlot (Mentor)**[2]

[1]**Idaho National Laboratory**
[2] **Ecole Polytechnique de Paris (Promotion X2020)**

May, 1^{st} **2023 - August,** 18^{th} **2023**

Idaho National Laboratory
Computational Frameworks
Idaho Falls, Idaho 83415

http://www.inl.gov

Prepared for the
U.S. Department of Energy
Office of
Under DOE Idaho Operations Office
Contract DE-AC07-05ID14517

Page intentionally left blank

Declaration of integrity regarding plagiarism

I, the undersigned Sixte M. de Boisset, certify on my honor:

1. That the results described in this internship report are the outcome of my work.
2. That I am the author of this report.
3. That I have not used other references or results without clearly citing and referencing them in accordance with the recommended bibliographic rules.

I declare that this work cannot be suspected of plagiarism.

Date: July 13th, 2023

Sixte M. de Boisset

Abstract

The aim of this study is to develop a model of a small High Temperature Gas cooled Reactor (HTGR) including the balance of plant. This microreactor produces electricity using the thermal power of the nuclear reaction. This work utilizes the MOOSE Multiphysics simulation tools, which are mainly developed at Idaho National Laboratory (INL, Idaho, United States of America). Its thermal-hydraulics and Heat conduction Modules are used to study the fluids behavior in the primary loop and power conversion system and their interactions with the heating structures. More specifically, one verifies that the temperatures, pressures and mass flow rates of the fluids in both loops are consistent and that, at the same time, all the power transfers occur as expected. Moreover, the various mechanical components characteristics (turbine, compressor, pump) are adapted to the reactor operating conditions. This first analysis is conducted using a simplified and one-dimensional model for the core. Ultimately, the obtained results are used to build a higher fidelity core model. This step aims to verify that the initial simplified simulation is consistent with the three-dimensional core modeling. In addition, the calculated material temperatures are checked. This study provides a fairly complete model of the thermal hydraulic phenomena for a particular design of High Temperature Gas cooled Reactor.

CONTENTS

Page intentionally left blank

Acronyms

AGR	Advanced Gas cooled Reactor
BWR	Boling Water Reactor
EFPY	Effective Full Power Year
FSV	Fort Saint Vrain nuclear reactor
GCR	Gas Cooled Reactor
HTGR	High Temperature Gas cooled Reactor
HTGTR	High Temperature Gas cooled Test Reactor
INL	Idaho National Laboratory
MOOSE	Multiphysics Object Oriented Simulation Environment
ORNL	Oak Ridge National Laboratory
PWR	Pressurized Water Reactor
SMR	Small Modular Reactor
TRISO	TRistructural ISOtropic fuel particle
UNGG	"Uranium Naturel-Graphite-Gaz" (Natural Uranium-Graphite-Gas) Reactor
VHTR	Very High Temperature Reactor
We	Watt of electrical power
Wth	Watt of thermal power
1D	one-dimensional
3D	three-dimensional

Page intentionally left blank

INTRODUCTION

The fluid choice in a nuclear power plant is a major field of study. The goal is to bring the thermal heat from the nuclear core to a turbine. Most of the designs use two loops. A primary coolant is heated by the fuel and transfers this power to a secondary fluid which induces the turbine rotation and consequently the electricity production by a generator.

In the case of a two loops reactor, the secondary loop fluid choice depends mainly on thermodynamic constraints and performance targets. On the other side, the primary loop coolant must respect various properties, including its effects on the nuclear reaction. Consequently, multiple reactor designs have been tested, depending on the coolant fluid choice. Many of them are water cooled, but other options exist like liquid metal, molten salts or gases.

Interest about the High Temperature Gas Cooled Reactor (HTGR) has grown for some years. This principle can be adapted to small size units and is consequently one of the possible designs for Small Modular Reactors (SMR). It provides high temperature gas, which can be deeply valuable when considering the new possible usages of nuclear energy. The high temperature property can increase the efficiency for an electrical power plant, but the thermal power can also be used for industrial heat or hydrogen production.

A set of technical specifications has been developed by the Pele program. The goal is to develop SMRs for military usages. These constraints have been adopted by E. M. Duchnowski et al. in [1]. In this study, they have developed a core design for a modular HTGR that is used in this work as design basis.

The goal of the following study is to develop a relatively complete thermal hydraulic and heat conduction simulation of a small HTGR. A one-dimensional simulation of the primary and secondary loop is firstly built, and then a three-dimensional core model is created. This is done step by step: a single assembly is first and foremost simulated, simplified to reduce the numerical cost and finally used to build the complete core. All these steps are done using the MOOSE Multiphysics simulation tools, which are developed at Idaho National Laboratory. Beyond the construction of this reactor model, this study aims to prove the possibility to build a consistent simulation of a HTGR using the MOOSE numerical tools. Consequently, this work answers to the following questions:

- What are the operating conditions provided by the one-dimensional numerical simulation, and are they consistent with the expected values?
- Do the results of a single assembly under the operating constraints defined in the one-dimensional simulation seem to be realistic, especially the materials temperatures?
- Does the complete core simulation provide consistent results with those obtained in the one-dimensional simulation and the single assembly model?

1 Problem statement

1.1 Context of this study

This study is about a High Temperature Gas cooled Reactor (HTGR). This reactor design is considered since few years as a promising technology, especially in the field of the Small Modular Reactors (SMR).

1.1.1 First generation gas cooled reactors

The HTGR design is relatively recent, but it is not the first type of Gas Cooled Reactor (GCR). The first nuclear industries based on this concept were developed mainly in the United Kingdom and in France. They were among the first generation nuclear reactors.

Both system were two loops' plants with a carbon dioxide cooled reactor. The French ones were called Natural Uranium-Graphite-Gas (UNGG) reactors and the British ones Magnox reactors, because of the magnesium alloy used to clad the fuel. The first reactor based on this principle, built at Calder Hall, is considered as the world's first nuclear power station.

General information about both designs is reported in Table 1 from a technical report of D. E. Shropshire for INL [2]. The Advanced Gas cooled Reactors (AGR) are discussed later.

Table 1: general information about the first carbon dioxide cooled reactors

	UNGG	Magnox	AGR
Number of reactors	8	26	14
Start year of the first reactor	1959	1956	1976
Shutdown year of the first reactor	1994	2015	2024 (estimated)
Power range (MWe)	80-995	200-1180	1200-1320
Nuclear fuel	Natural uranium	Natural uranium	low enriched uranium
Moderator	Graphite	Graphite	Graphite
Primary coolant	CO_2	CO_2	CO_2

Both systems were constantly improved. Consequently, each reactor or pair of reactors operating parameters differed. Moreover, the British system had a bigger development and led to new reactor designs. Thus, and as an example, only the operating values of the Calder Hall reactor are given in Table 2, where they are compared to the next British GCR. These data come from [2].

These reactors presented many assets, including the possible use of non-enriched nuclear fuel and the negative power coefficient of reactivity. It means that a rise of the temperature would induce a decrease in the reaction rate, provoking a natural equilibrium.

Because of the use of natural uranium, the power density was nevertheless small and induced large scaled nuclear cores and lower production than the widespread Pressurized Water Reactors (PWR) or Boiling Water Reactors (BWR), which are the main current designs and provide generally around 1 GWe per reactor.

The fuel was natural uranium (non enriched in fissile uranium isotope), inserted in metallic clads and put in graphite blocks for the moderation.

1.1.2 Second generation gas cooled reactors

If the GCR represented a large amount of the first generation nuclear reactors, many of the second generation ones were PWR or BWR. For instance, France abandoned its UNGG industry and developed PWR plants.

Nevertheless, the success of the British Magnox and the need of more compact reactors led to the development of the Advanced Gas cooled Reactor (AGR). This new system uses low enriched uranium, which are also inserted into metallic clads among a nuclear moderator. Consequently, their production is higher than for Magnox reactors, as shown in Table 1.

The Calder Hall and Chaplecross (Magnox design) operating values are compared in Table 2 with those of Hinkley Point B (AGR design). The second system reactors were more similar together, so this example can be considered as relatively representative.

Table 2: operating parameters of the Calder Hall and Hinkley point B nuclear reactors

	Calder Hall (Magnox)	Hinkley Point B (AGR)
Power (MWe)	220	1250
Efficiency	$\sim 30\%$	$\sim 40\%$
Primary pressure (bar)	6.9	42
Core outlet temperature (K)	609	913
Clad temperature (K)	~ 773	~ 1155
Limit fuel temperature (K)	≤ 923	≤ 2273

The enrichment and cladding changes made it possible to increase the fuel and clad limit temperature, leading to higher operating temperatures. The power density was consequently increased and the plant production once again higher. The fluid pressure is increased to make it possible to the coolant to bring this bigger thermal power.

Another historically important design was implemented at the Fort Saint Vrain (FSV) nuclear power plant (United States). This reactor was commercially operated between 1979 and 1989. It followed a prototype, the Peach Bottom reactor, with some structural and operating differences. Its main operating parameters are reported in Table 3, from D. Copinger et al. [3]:

Table 3: operating parameters and general information about the FSV nuclear reactor

Power (MWe)	330
Efficiency	$\sim 40\%$
Fuel type	combination of uranium and thorium
Moderator	Graphite
Primary coolant	Helium
Primary pressure (bar)	48
Core outlet temperature (K)	1050

The Fort Saint Vrain reactor used prismatic graphite fuel assembly, in which fuel rods are inserted. These ones are constituted of a carbonaceous matrix surrounding the fuel particles coated with pyrolytic carbon and silicon carbide.

The main change about the thermal hydraulic processes is about the coolant fluid. Fort Saint Vrain reactor used helium instead of CO_2. No gas presents perfect properties in terms of safety,

low neutron absorption, inertness and thermodynamic properties. Nevertheless, Helium is an inert gas with good heat transfer properties.

These two GCR reactor designs are important in term of inspiration. The quoted Idaho National Laboratory (INL) reference [2] about the Magnox, UNGG and AGR points out the feedbacks provided by these industrial systems. In the case of the FSV nuclear plants, feedbacks were listed in [3] by the Oak Ridge National Laboratory (ORNL) which operated experimental tests from 1981 to 1989.

1.1.3 Fourth generation HTGR

The main nuclear reactor types among the second and third generations of nuclear reactors are the PWR and BWR. Nonetheless, for some years, new interest has been growing about other possible designs. Among the motivations, new usages of nuclear power are considered, as industrial heat or hydrogen production. In these fields, higher temperature reactors present some assets, including High Temperature Gas cooled Reactors (HTGR).

This type of reactor presents also strong assets in term of safety. As for the previous GCR, its reactivity temperature coefficient is negative. Its fuel is based on TRistructural ISOtropic (TRISO) fuel coated particles, which should not melt. These particles are constituted of a fuel kernel surrounded by multiple silicon and carbon layers, with a total radius about 0.5 mm.

As for the FSV design, helium is defined as primary coolant.

Two main designs are being developed: the pebble bed reactor and the HTGR using prismatic fuel assembly.

The pebble bed reactor uses TRISO particles inserted in graphite pebbles whose size is like a tennis ball. This ball can move in the primary loop, and the fuel is consumed in the core. In that place, a critical mass which allows the nuclear reaction is reached. The main asset of this design is that the fuel can be recharged online.

The principle of the prismatic assembly type is close to FSV fuel composition [3]. Once again, fuel assemblies are prismatic graphite blocks. The hexagonal apothem of the hexagon is about few centimeters to few tens of centimeters. Tens of fuel and coolant channels are inserted in the assembly. The fluid goes through the second ones, and a fuel material is put in the first ones. It is constituted of TRISO particles inserted in a graphite matrix.

Some other fuel types are considered, as a Silicon matrix fuel in the study of C. Lu et al. [4]. This one would have a better nuclear particles retention and would make possible to reach highest fuel temperatures. In the same vein, other moderators are tested to replace graphite (E.M. Duchnowski et al.,[5] and [1]). Its drawbacks are in particular: non uniform expansion and contraction under irradiation, and lower discharge burnups and cycle length than with other moderators. Nevertheless, graphite is a more widespread and known material: it will be considered in the following study as moderator and matrix material, with its own thermodynamic properties.

Some prismatic HTGR are presented below:

- The Very High Temperature Reactor (VHTR)

The VHTR is a fourth-generation reactor project (D.L. Mose, [6]. Web site of the Generation IV international forum, [7]). It should be a helium cooled reactor using a graphite moderator. It

could produce electricity using a Brayton or Rankine cycle as secondary loop. Both pebble bed and prismatic designs are considered. The second one is presented in this section.

Multiple designs are being developed. The general operating parameters are reported in Table 4, from [6] and [7]:

Table 4: operating parameters of the VHTR

Power (MWth)	200-600
Efficiency	40% - 50%
Core inlet temperature (K)	500 - 940
Core outlet temperature (K)	1020 - 1280
Primary pressure (bar)	50 - 90

- The High Temperature Gas cooled Test Reactor (HTGTR)

A High Temperature Gas cooled Test Reactor (HTGTR) design has been developed at Idado National Laboratory (INL) using the RELAP simulation tools (J.W. Sterbentz et al., [8]). They are derivated from the MOOSE tools, which will be presented in 1.2 and are used in this study. The goal of the simulation of the HTGTR is to build a test reactor design, while the United States have no more operating HTGR. This design uses multiple feedbacks coming from the FSV nuclear power plant and the AGR. The operating parameters are presented in Table 5.

Table 5: operating and geometrical parameters of the HTGTR

Power (MWth)	200
Core inlet temperature (K)	600
Core outlet temperature (K)	920
Peak fuel temperature (K)	~ 1520
Primary pressure (bar)	70
Mass flow rate (kg/s)	117
Core height (m)	9.2
Active core height (m)	6.4
Core diameter (m)	3.4

This reactor is a large scale one, with important geometrical dimensions which are reported in Table 5. They are deeply larger than the typical size of the reactor studied in this work, which is closer to the designs presented in the last paragraph.

- Small Modular HTGR

The interest about small modular reactors has grown during the last years. One reactor possible design is the HTGR. Among others, the Pele program provides technical specifications about a nuclear reactor which could be used for military purposes. They are reported in Table 6 [1].

Many different proposed designs have been developed. E.M. Duchnowski et al. [1] present a particular reactor model using prismatic assemblies and with a core pattern inspired by the FSV feedbacks. This example will be the design basis of the following study.

Table 6: Pele program technical specifications

Parameter	Objective
cycle length	$\geq$ 3 years at 100% without refueling
Power (MWe)	1-10
Size	must fit in a container
Fuel type	High Assay, low-Enriched Uranium (HALEU) TRISO particles

1.2 Simulation tools

MOOSE (Multiphysics Object-Oriented Simulation Environment) is a finite element framework. It has been developed at Idaho national Laboratory (INL). It is divided between multiple apps and modules used to simulate different types of phenomena: thermal-hydraulics, heat conduction, material behavior or neutronics among others. These tools can be coupled to simulate complex problems, such as a nuclear core behavior, which is a Multiphysics problem. The modeled objects can be in one, two or three dimensions. The latest option gives more precise results but has a higher simulation cost. When it is possible, the components are modeled using one- or two-dimensions tools to simplify the numerical problem.

1.3 Problem presentation

The simulated reactor is a HTGR (High Temperature Gas cooled Reactor). Its thermal power is 15 MWth, and the generator must produce 2 MWe. The system couples a helium-cooled primary loop with a Brayton cycle. It is illustrated in Figure 1, and the operating conditions are provided in Table 7. These ones are the values measured with the finished simulation. Except the core and generator powers, most of them were not precisely defined at the beginning but were adapted during the construction of the model. Nevertheless, the initial estimated values for these parameters were close to the final results which are given in this table.

Table 7: Operating conditions

Operating Conditions	
Total core power	15 MWth
Primary mass flow rate	9.4 kg/s
Core inlet temperature	890 K
Core outlet temperature	1190 K
Primary system pressure	9 MPa
Secondary mass flow rate	20 kg/s
Secondary heat exchanger inlet temperature	490 K
Compressor pressure ratio	8.9
Turbine pressure ratio	4.1
Generator power	2 MWe

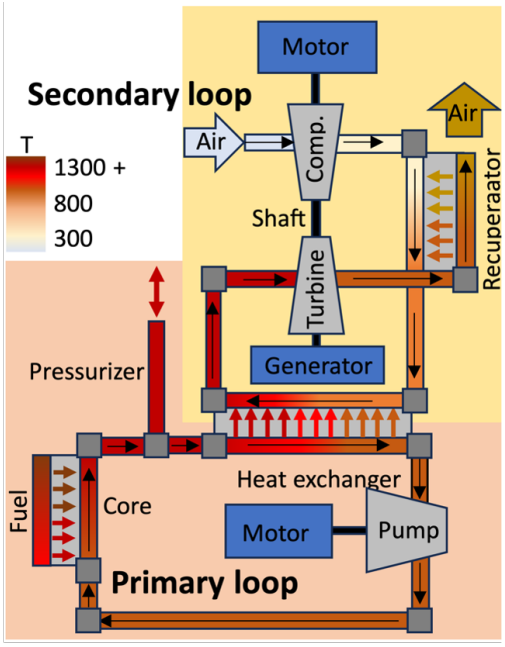

Figure 1: System diagram

1.3.1 Primary loop

The primary loop consists of a core, a heat exchanger and a pump to compensate the pressure drop. Helium is a common coolant among HTGRs because of its inert gas properties. The primary core temperatures given in Table 7 are consistent with those presented in 1.1.3. The core inlet fluid temperature is about many hundreds of Kelvin degrees but smaller than 1000 K, and the outlet core fluid temperature can be about 1200 K in some designs. In the same vein, the primary pressure is comparable to the biggest considered values for the VHTR.

The core design is copied on [1]. It is composed of 55 hexagonal fuel assemblies. Their geometrical characteristics are given in Table 8. The assembly and the core patterns are provided in Figure 2a and Figure 2b. Duchnowski et al. [1] consider a simplified model. Consequently, the core barrel and pressure vessel are not taken into account.

Some of these parameters are not defined but tested in [1] among a wide range of values, including the lattice pitch, the type of TRISO particles which constitute the fuel in a graphite matrix and the packing fraction of these fuel particles in the matrix. The thermal power is also tested between 2 and 20 MWth.

The authors build simulations for lattice pitches between 1.5 and 2.5 cm. Below 1.5 cm the fuel and coolant channels overlap, and the core diameter limits the size of the assembly and consequently the lattice pitch.

The TRISO particles are UN or UCO TRISO particles, containing different proportions of fuel, graphite and layer materials, and have different radius. Their typical sizes are therefore almost similar (their radii are about 0.5 mm).

Finally, different packing fractions between 0.1 and 0.5 are tested. It represents the volume proportion of fuel particles among the graphite matrix.

Table 8: Primary loop parameters

Component	parameter	value
Fuel channels	radius	0.00794 m
-	number per assembly	42
-	matrix material	Graphite H-451
-	UN TRISO packing fraction	0.5
Coolant channels	radius	0.00635 m
-	number per assembly	18
-	coolant gas	Helium
Assembly	lattice pitch	0.022 m
-	height	2 m
Core	radius	0.9 m
-	number of assemblies	55

(a) Assembly

(b) Core

Figure 2: Patterns

The goal of their study is to compute the discharge burnup and the cycle length in function of the lattice pitch, the type of particles, the packing fraction and the thermal power. The moderator is graphite.

In every case, better results are got with UN TRISO particles. Consequently, these ones are selected for the following study.

The cycle length and discharge burnup are improved with a high lattice pitch. Thus, a value of 2.2 cm is selected, which is among the highest possible ones, but it also lets a margin under the core diameter limit.

The discharge burnup is better for a small packing fraction, as shown in Figure 3a, but the cycle length is bigger for the highest packing fraction values, as shown in Figure 3b. The fuel consumption is optimal when the fuel amount is smaller, but it also reduces the cycle length. The packing fraction choice depends on the fuel cost. It is negligible, consequently the cycle length is the main parameter to optimize. Thus, the packing fraction is defined at 0.5. Finally, as shown in Figure 3c, the cycle length seems to depend mainly on the power and few on the packing fraction.

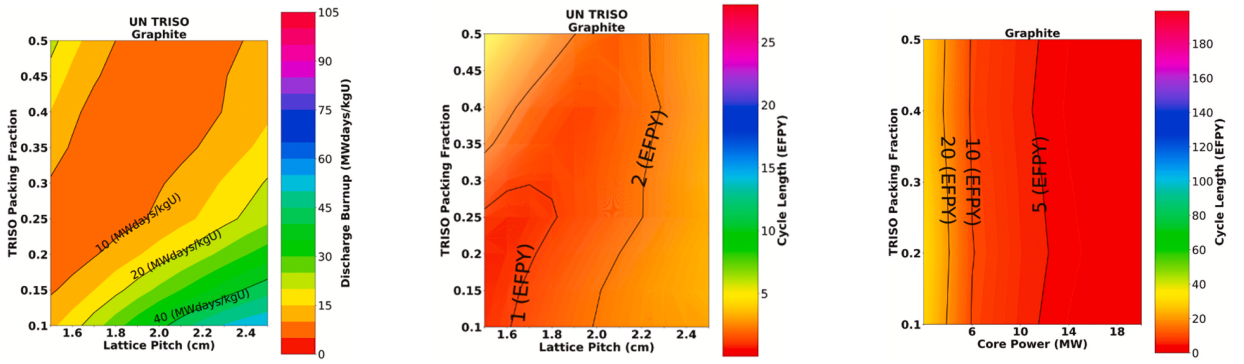

(a) discharge burnup for various lattice pitch and packing fraction values

(b) cycle length for various lattice pitch and packing fraction values

(c) cycle length for various power and packing fraction values

Figure 3: contour plots of the cycle length and discharge burnup for various power, lattice pitch and packing fraction values and with UN TRISO as fuel (plots from [1])

A value of 15 MWth is selected. This is a typical thermal power value for this type of reactor, and leads to a not too small cycle length, about few Effective Full Power Years (EFPY).

Some of these parameters are not directly thermal hydraulic or heat conduction properties, such as the TRISO particles type or the packing fraction. They are nevertheless used to compute average values of thermodynamic and density homogeneous properties of the fuel channels, constituted of fuel particles and graphite matrix, which are then used to solve the heat conduction problem.

1.3.2 Secondary loop

The secondary loop is an open recuperated Brayton cycle, which is presented in the MOOSE resources [9] (open-source reference). A Brayton cycle is a thermodynamic system which transforms thermal into mechanical power. The general principle is the following, and is illustrated by the diagrams in Figure 4:

- Step 1: a gas is compressed during an adiabatic and isentropic step.
- Step 2: it undergoes an isobaric heating.
- Step 3: the gas is decompressed in a turbine. This step is once again adiabatic and isentropic.
- Step 4: the gas undergoes an isobaric cooling to eliminate the residual thermal power from the gas.

The simulated Brayton cycle is called open and recuperated. It has the following supplemental properties:

- Step 4 is virtual. The gas is air, taken from the atmosphere and finally released outside. It is equivalent to an isobaric cooling of the fluid. Nevertheless, no supplemental cooling system is needed.

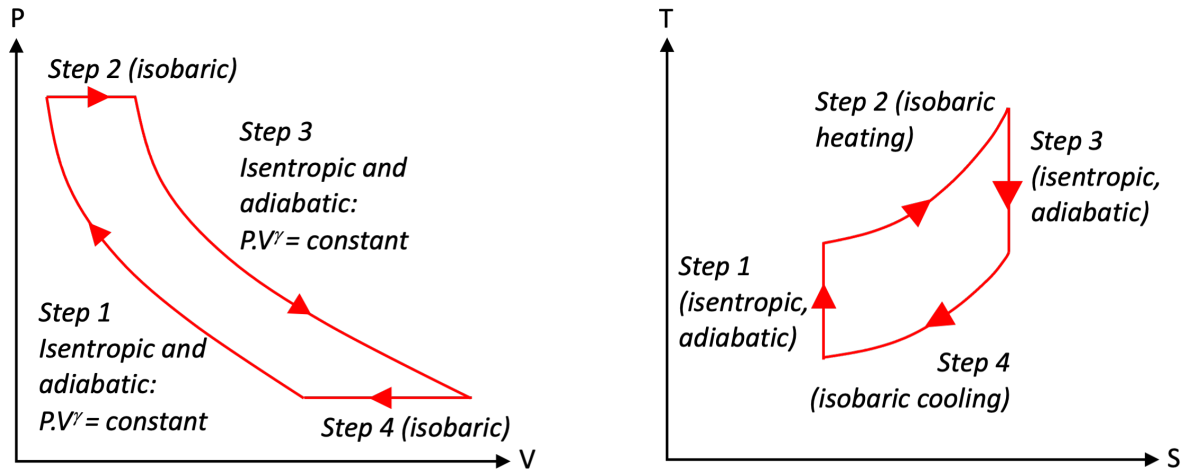

(a) pressure - volume diagram

(b) temperature - entropy diagram

Figure 4: PV and TS diagrams of the ideal Brayton cycle

- Before being released outside, the exhaust gases coming from by the turbine transfer a part of their thermal power in the recuperator (see Figure 1) to the inlet gases, before they are heated again by the heat source. This supplemental step increases the efficiency.

The adiabatic property of Steps 1 and 3 is by construction respected. The heat transfers are considered in the simulation only in the core, in the heat exchanger and in the recuperator. The isentropic property is more difficult to verify. The isobaric property will be checked in 2.3.1.

Because of its openness to the atmosphere, the pressure in the secondary loop components is about few bars. By contrast, the temperatures are comparable to those of the primary loop. The air at the inlet has an atmospheric temperature but is deeply heated in the heat exchanger.

Some system characteristics must be highlighted. All the mechanical components of the used Brayton cycle are on the same shaft. It is shown by Figure 1: a motor, the compressor, the turbine and a generator rotate on a common shaft. The first and the last components have no role in the steps defined above. They are presented below.

The generator extracts mechanical power and transforms it into electrical power. That is the reason why this component is on the same shaft than the turbine: this one receives thermal power from the gas, and the gas expansion generates its rotation, transmitted to the generator by the shaft.

A motor is added to the system. In a steady state, the Brayton cycle must operate autonomously and receives no external power, except the heat provided during step 2. The turbine and the compressor are on the same shaft: thus, the turbine rotation is transmitted to the compressor and provides its necessary input power. Consequently, the motor is useless during the steady state. Nonetheless, the system needs to be launched at the beginning. Initially, the motor provides a torque which provokes the shaft rotation and consequently the compressor (and turbine) start-up. Thus, the compressor generates the gas flow in the cycle. When the steady state is reached, the motor is shut.

1.4 Simulation tools used in this study

The goal of this study is to simulate the thermal hydraulic and heat conduction behaviors of the presented HTGR. The provided power is considered as a constant, and the solid materials do not deform. The heat conduction phenomena are mainly located in the core, on both sides of the heat exchanger and in the recuperator. The two latest components are simulated using one and two-dimensional tools from the Thermal hydraulic Module (open-source). The core is firstly simulated using these ones, in order to build the other components of the primary loop and adapt them to the operating conditions. Then, a more precise simulation of the core is done using the Heat conduction Module (open-source) and coupled to the thermal hydraulic problem.

2 1D thermal hydraulic simulation of the primary and secondary loops

2.1 Equations

The MOOSE Thermal hydraulic Module (open-source) is used to model the primary and secondary loops. It solves the three conservation equations of mass, momentum and energy, applied on a 1D geometry, with a single-phase, inviscid, compressible and area variable flow. These equations are given below:

Mass equation: $\frac{\partial A\rho}{\partial t} + \frac{\partial A\rho v}{\partial t} = 0$
Momentum equation: $\frac{\partial A\rho v}{\partial t} + \frac{\partial A\rho v^2}{\partial z} = Af - A\frac{\partial p}{\partial z} + CF_p$
Energy equation: $\frac{\partial A\rho(e+\frac{v^2}{2})}{\partial t} + \frac{\partial A\rho v(h+\frac{v^2}{2})}{\partial z} = Afv + Cq_p$

where A is the area, C the heating perimeter, ρ the density, v the velocity, f the volume force, p the pressure, e the energy, h the enthalpy and q_p the heat transfer.

These equations depend on three unknowns: the pressure, the temperature and the velocity, which are space and time dependent. Fluid state laws are added in the simulation to complete the resolution system. Two terms are nevertheless unknown: the friction factor and the heat flux, which can be written as:

$q_p = h(T_c - T_f)$, where T_c and T_f are respectively the hot and cold sides temperatures, and h is the heat transfer coefficient.

These terms appear in the simplification from the 3D to the 1D-conservation equations. They can be modeled using non-dimensional parameters:

$$\frac{CF_p}{A} = -\frac{1}{2D_h} f(R_e)\rho|v|v$$

$$h = \frac{\lambda}{D_h} Nu(R_e, P_r)$$

where D_h is the hydraulic diameter of the channel, λ is the thermal conductivity, R_e is the Reynolds number and P_r is the Prandtl number. $f(R_e)$ is the Fanning friction factor and $Nu(R_e, P_r)$ is the Nusselt number, and both of them can be determined using models.

f and h are defined using experience-based models. In this study, two steps are performed:

- Initially, the friction and heat transfer coefficients are considered as constant values. This simple model is applied using a simple closure tool. The goal of this step is to be able to adapt the components, fluid and material properties as the operating parameters in order to reach results as close as possible to the theoretical values using a not too complicated numerical problem.
- The simulation is enhanced using experience-based models. The results provided in this report are computed using this method.

In the second case, both terms are computed as follow:

- The friction factor is defined using the Churchill experience-based model:
  $f = 2.0\left(\left(\frac{8}{Re}\right)^{12} + \frac{1}{(a+b)^{1.5}}\right)^{\frac{1}{12}}$
  with $a = \left(2.457 \ln\left(\frac{1.0}{(7/Re)^{0.9}}\right) + \frac{0.27\epsilon}{D_h}\right)^{16}$ and $b = \left(\frac{37\,530}{Re}\right)^{16}$ and where ϵ is the wall roughness.
- The Nusselt number is computed using the Dittus-Boelter experience-based model:
  $Nu = 0.023 Re^{4/5} Pr^{0.4}$

These two models are currently the two only ones accessible in the MOOSE Thermal hydraulic Module.

2.2 Construction of the system

Each component and then loop is built separately and in a second step coupled with the other elements. This method is applied to be able to detect quickly simulation issues and to adapt each part of the system to the wanted operating values before to connect them together. A connection of all the components and loops without these intermediate steps would probably result in a simulation fail.

2.2.1 Core model

The core is initially modeled as a 1D-coolant channel. It is replicated $18 * 55$ times, which is the number of coolant channels per assembly multiplied by the number of assemblies. This channel is surrounded by a hollow graphite cylinder, which is itself in a hollow fuel cylinder. The outer radii of these two cylinders are computed considering the average amount of graphite and fuel around each coolant channel.

It is a temporary simulation of the core, used to build a closed primary loop and adapt it to the operating values. It will be in a following step replaced by the 3D heat conduction model of the core.

Consequently, this model does not need to be perfectly defined in term of temperature dependence of the material properties. The specific heats and thermal conductivities of the fuel and graphite are considered as constant values. The properties of the fuel are considered to be the same than the uranium properties and are adapted to more accurate values in the 3D core model.

2.2.2 Adaptation of the secondary loop

The next primary loop construction step would be to define the heat exchanger. The inlet and outlet temperatures on the primary side are almost known. The helium temperature is initially the same than at the core outlet and its value at the heat exchanger exit is almost like the inlet core temperature, because we expect that the compression in the primary pump will not induce a deep temperature change. Nonetheless, most of the operating values presented in Table 7, including the inlet and outlet temperatures on the secondary side, are not precisely known and will be completely defined when the simulation will be finished. They need to be computed to build the heat exchanger. Consequently, the secondary loop is firstly defined, and its operating temperatures will be next used to build the complete heat exchanger.

To do that, an already existing simulation of an open recuperated Brayton cycle, defined in 1.3.2 and whose complete documentation is available on [9] (open-source MOOSE resources), is

firstly adapted to receive 15 MWth and produce 2 MWe. The heat exchanger in this loop is modeled as a coolant channel which receives an imposed thermal power from a heat structure.

First and foremost, an estimation of the secondary mass flow rate can be determined. The fluid which enters the heat exchanger has been heated by the initial compression and the recuperator. We assume an increase about few tens of degrees, but no more than 200 K. We consider an inlet temperature about 500 K. Then, using the following equation, an estimation of the mass flow rate can be determined:

$\Delta P = \dot{m} C_p \Delta T$, with $\Delta P = 15$ MWth, $T_{inlet} \approx 500$ K, $T_{outlet} \approx 1200$ K and $C_p(air) \approx 1000$ J/(kg.K)

Thus, $\dot{m} \approx 20$ kg/s

Consequently, the system must obey to two constraints. First, the mass flow rate must be enough high to carry the power provided by the primary loop, at least 20 kg/s. Secondly, the generator must provide 2 MWe, as defined in the operating values.

Three components need to be adapted: the generator, the turbine and the compressor. The behavior of the two last ones is defined by their rated parameters, which are computed above, and their performance curves. These ones are taken from D.P. Guillen et al. [10].

The extracted power from the generator follows these equations:

$\Gamma_{generator} = C\omega_{shaft}$, with $\Gamma_{generator}$ the generator torque and ω_{shaft} the radial shaft speed,
$P_{generator} = \Gamma_{generator}\omega_{shaft}$, with $P_{generator}$ the generator power.

The following value is affected to the constant C:

$C = 0.025 W.s^2$

Consequently, a shaft speed can be computed and is added among the compressor and turbine rated parameters. The rated densities and sound speeds are computed using the MOOSE tools and the expected pressure and temperature operating conditions. All these parameters are shown in Table 9 and compared to steady state values.

Table 9: Compressor and turbine rated values

Component	values	ρ (kg/m3)	ω_{shaft} (rad/s)	sound speed (m/s)	$\dot{m}$ (kg/s)
Compressor	rated	1.2	9948	340	20
-	steady state	0.8	9329	330	20.5
Turbine	rated	1.4	9948	670	20
-	steady state	1.43	9329	676	20.5

The shaft speed is significantly smaller than the rated value. This value is controlled by retroaction tools which impose it to reach the wanted shaft speed value. This one is in fact smaller than the rated value and is fixed at 9000 rad/s. This additional condition is imposed to avoid damages on the turbine and compressor if the shaft speed exceeds the rated value.

The rated density and sound speed of the compressor differ also from the steady state values. It is due to a deep decrease of the pressure at the entry of the compressor. It gets atmospheric air

at rest, which gains an important velocity at the compressor inlet. Consequently, because of the Bernoulli relation (stationary, inviscid and incompressible flow),

$$\frac{p}{\rho} + \frac{v^2}{2} + gz = constant$$

the pressure decreases. It also induces the same evolution on temperature, because of the ideal gas property of the air. That effect explains the difference with the rated values, which are the density and sound velocity at the atmospheric conditions.

Finally, the pipes diameter is adapted. A typical pipe diameter would be around 0.25 m, which is equivalent to one foot (imperial system). Nevertheless, it would lead to a fluid velocity near the sound velocity at the atmospheric conditions and would consequently induce compressible effects at the compressor inlet. In order to avoid this issue, the pipe diameter is increased at 0.35 m, which is still consistent with the typical size of the pipes for this type of small reactors.

The adaptation of the secondary loop provides the heat exchanger temperatures, mass flow rate and pressure on the secondary side which will be used to build the model of this component.

2.2.3 Heat exchanger model

The heat exchanger is modeled using 20,000 couples of 2 m high primary and secondary channels, separated by a 1 mm thick steel wall. The flows are on the opposite directions, in order to maximize the heat exchange. The boundary conditions come from the secondary loop adaptation for the secondary side, and from the core model for the primary side.

2.2.4 Primary pump model

The primary loop pump must compensate the pressure drop in the heat exchanger and in the core. In order to have an estimated value, the core and the primary side of the heat exchanger are coupled. The corresponding pressure drop is measured at 0.17 bar.

Five rated values must be defined for the pump: the density of the fluid, the volumetric flow rate, the pump torque, the shaft speed and the pump head. These values are computed as follow:

- The temperature in the pump is about 890 K and the pressure is 90 bar. Around these operating values, the helium density is approximately 5 kg/m^3 (computed using the MOOSE tools).
- The mass flow rate is about 9.35 kg/s. Consequently, using the fluid density, the volumetric flow rate is approximately equal to 2 m^3/s.
- The head rated is defined as the fluid column which would have the same hydrostatic pressure at its bottom. Thus, it is defined as: $H = \frac{\Delta p}{\rho_{He} g} \approx 350m$
- The gain of power in the pump is about 200 W. Because of the relation between the shaft speed, the torque and the power, a torque and shaft speed couple can be determined. It is initially fixed at 40 N.m and 5 rad/s, but the torque value is increased to 50 N.m to make the simulation run easier.

A comparison between the rated values and the steady state values that are got in the entirely coupled primary loop (next step) is provided in Table 10:

Table 10: Pump rated values

values	ρ (kg/m^3)	$\dot{V}$ (m^3/s)	H (m)	ω_{shaft} (rad/s)	Γ_{pump} (N.m)
rated	5	2	350	5	50
steady state	4.86	1.92	293	4.5	42

2.2.5 Connection of the primary loop components and with the secondary loop

All the primary loop components are linked with pipes. Their typical diameter is fixed at 0.25 m (approximately one foot). Some small adjustments are performed. Among them, a pressurizer is added in the primary loop, between the core and the heat exchanger, and imposes a 90 bar pressure value. HTGRs normally contain no pressurizer, but this component is defined to avoid a non-desired pressure increase during the transient period in the primary loop. There is no way to control the gas amount during this step using the simulation tools. Because of the Ideal Gas Law and because of the core heating, the primary pressure would increase far away from the operating value. The pressurizer is added to avoid this phenomenon.

Finally, the two loops are coupled by the heat exchanger. Once again, the input file undergoes small adjustments to reach the operating values and optimize the simulation.

The initial conditions are imposed in order to be close to realistic values and in the same time to avoid irregular effects at the beginning of the simulation. Consequently, a common temperature of 400 K, which is close to the operating value in the secondary loop, is defined for the whole system. Thus, a too high initial temperature gap between the two loops on the heat exchanger is avoided. It would result in an initial and non-physical power exchange between the two sides before that the power emitted by the core would reach the heat exchanger.

By contrast, the initial pressures in the two loops have different values. The primary pressure, which must stay almost stable during the simulation, is initialized at its operating value. On the contrary, the initial secondary pressure is equal to the atmospheric pressure because the compressor and the turbine are initially at rest and the Brayton cycle is opened on the atmosphere.

Finally, the initial velocities are fixed at zero.

2.3 Results of the simulation

Two situations are tested on the simulation coupling the two loops: a startup transient and a load follow transient.

2.3.1 Startup transient

In this simulation, a constant power is imposed in the heat structure of the core, and is equal to 15 MWth, which is the operating value. The system is initially at rest. The turbine and compressor shaft is launched by the motor, which is controlled by a retroaction tool. As presented in 2.2.2, the goal is to make the shaft speed reach a value a bit smaller than its rated value. To do so, the motor torque increases dramatically during the first few seconds and make the shaft reach a steady state in approximately 6000s. It launches the compressor and the turbine, while the motor torque decreases slowly to zero, as shown in Figure 5a.

The startup transient is run during 50,000 s, and a steady state seems to be reached around 20,000s, as shown in the following figures.

First and foremost, the power transfer must be verified. As expected, the transferred power in the core and consequently in the heat exchanger is at the beginning equal to zero and finally reaches its 15 MWth operating value. The generator power starts also from zero and increases to 2 MWe, which is the desired result. These results are plotted in Figure 5b

The primary loop pressure evolution is not represented in the following results, because it stays as expected around the imposed pressure value of 90 bar which is also the initial value. By contrast, a more sizeable evolution can be seen on the secondary side pressure, as plotted in Figure 5c. As expected, most of the measured values increase dramatically during 20,000 s and then reach a steady state.

The main pressure evolution takes place in the compressor, where it increases from a value close to the atmospheric pressure to 5.8 bar. The inlet pressure is smaller than 1 bar because of the fluid velocity, as presented before in 2.2.2.

The pressure drop in the channels and in the heat exchanger can also be determined: from the compressor outlet to the turbine inlet, it decreases slowly from 5.8 bar to 4.8 bar. Nevertheless, this pressure drop is small in the heat exchanger (approximately about 10%), which is close to the isobaric heating hypothesis in the heat exchanger, assumed for the Brayton cycle.

Finally, the turbine outlet pressure is close to the atmospheric pressure but differs because it is separated from the outlet by the recuperator.

The temperatures are plotted in Figure 5d. The steady state is once again reached in approximately 20,000 s. Helium is heated in the core from 890 K to 1190 K and transfers this thermal power in the heat exchanger to the secondary fluid. Air is heated from 490 K to 1170 K in this component. The outlet value is consistent with the fact that it cannot be bigger than the primary fluid higher temperature but at the same time can be this high because the primary and secondary flow channels have opposite orientations.

The wall temperature increases as expected in the core, because the coolant temperature increases at the same time. It stays under 1400 K.

These temperature values are consistent with those given in 1.1.3, which are about many hundreds of Kelvin degrees at the core inlet but smaller than 1000 K for the fluid, and can be bigger than 1000 K at the core outlet.

Ultimately, the steady state maximum and minimum values of the heat transfer coefficient between the wall and the fluid are measured. They are respectively 1466 and 1463 $W/(m^2.K)$. These values will be compared to those obtained for the 3D simulation in 3.4.2.

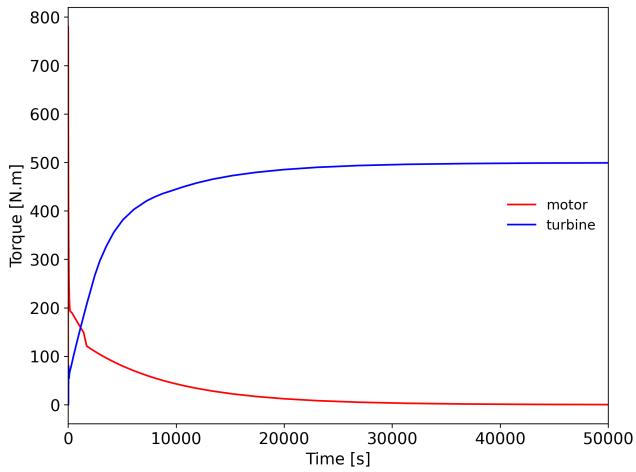

(a) turbine and motor torques

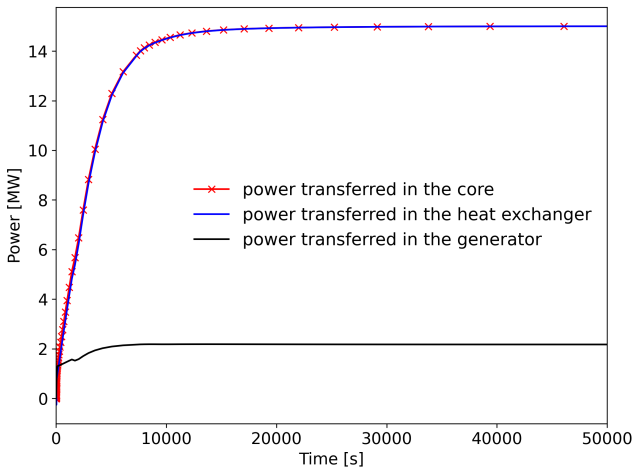

(b) core, heat exchanger and generator powers

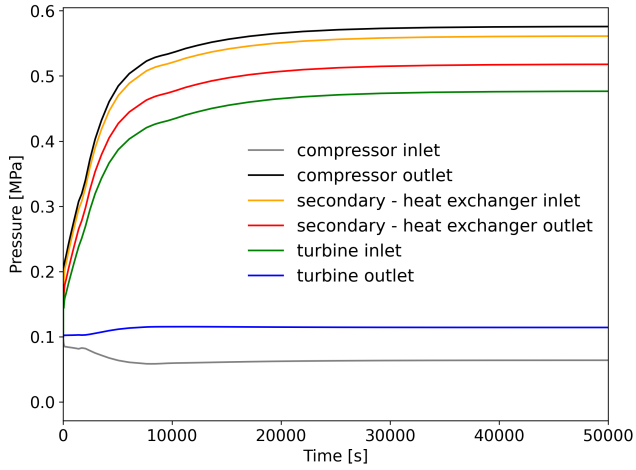

(c) pressure in the secondary loop components

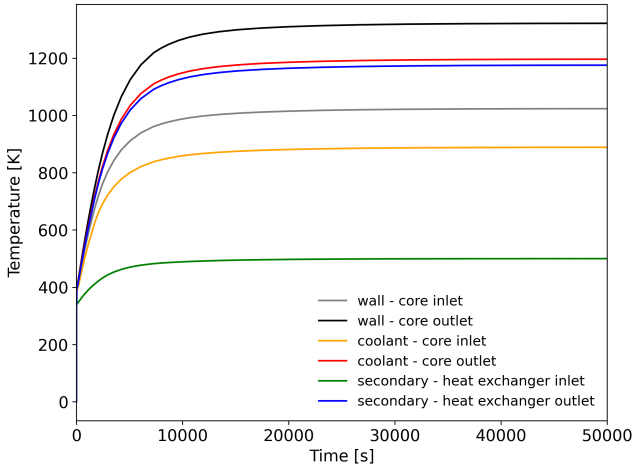

(d) temperatures in some components

Figure 5: results of the startup transient

2.3.2 Load follow transient

The ability of the simulated loops to react to a power change is also tested. In real life, this situation could correspond to a power modulation due to the evolution of the consumption.

The system is initially in a steady state. Consequently, the motor is initially and stays at rest during the simulation. The core power is maintained at 15 MWth from the beginning to 50,000 s, and then fixed at 80% of the operating value. It is finally defined again at 15 MWth after 100,000 s.

New steady states are reaches after 10,000 s for both modulations, as shown in Figure 6.

As expected, the modulation of the power provided by the heat structure of the core induces the same changes, after transient steps, on the power transferred to the primary fluid in the core and in the heat exchanger. It induces also a decrease of 20% of the extracted electric power: the generator power measures 1.6 MWe. It is illustrated in Figure 6a.

The temperatures are plotted in Figure 6b. Because of the lower power provided in the core between 50,000 s and 100,000 s, the gas temperatures are smaller. The helium flow temperature in

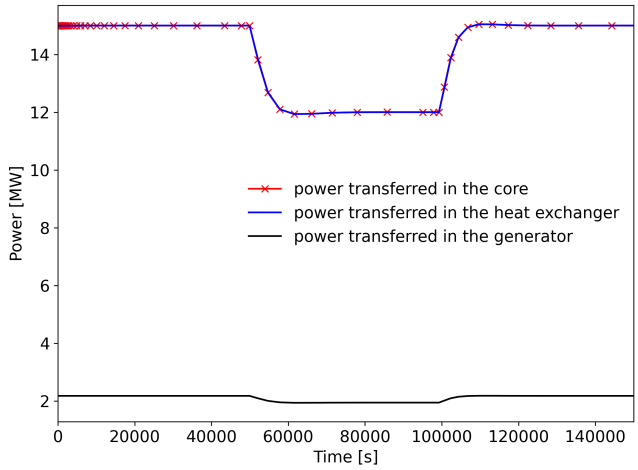

(a) core, heat exchanger and generator powers

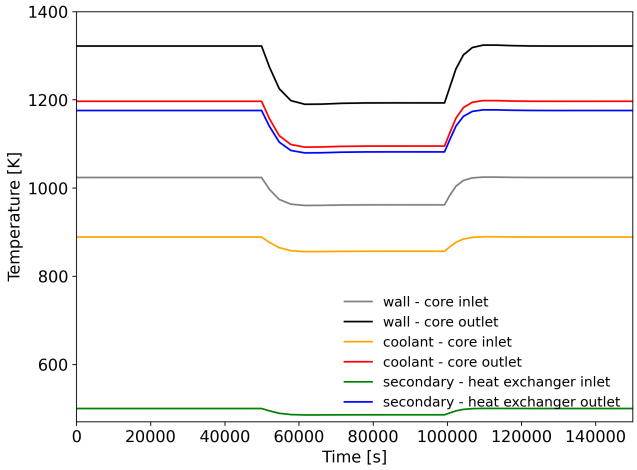

(b) temperatures in some components

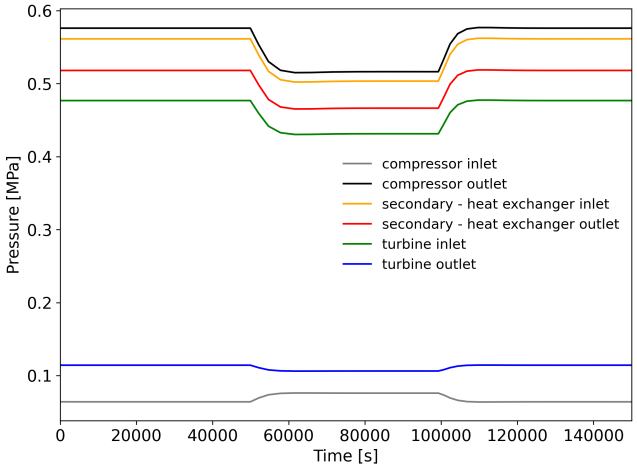

(c) pressure in the secondary loop components

Figure 6: results of the load follow transient

the core increases from 855 K to 1090 K and releases its thermal power to the secondary fluid in the heat exchanger. In this component, the air flow is heated from 480 K to 1080 K.

As expected, this power modulation has a minor effect on the temperature at the heat exchanger inlet. Its effect on the air before the heat exchange is in fact limited to its consequence on the shaft speed. This component links the turbine, which is impacted by the power modulation, and the compressor, which influences the air properties at the heat exchanger inlet.

Another steady state is reached after the second modulation, which is equivalent to the first one.

Finally, Figure 6c presents the pressures in the secondary loop. Because of the Ideal Gas Law and the lower temperatures due to the power modulation between 50,000 s and 100,000 s, the measured pressures are smaller during this step. They reach once again their initial values when the second modulation sets the core power to the normal operating value.

3 3D heat conduction simulation of the core

The next step is to build a 3D core model. It is divided into multiple sub steps:

- a single fuel assembly is modeled using the MOOSE Heat conduction Module and connected to the exact number of coolant channels per assembly, simulated using the MOOSE Thermal hydraulic Module,
- The coolant channels are reduced to only one for this single assembly. The results are compared with the previous simulation.
- 55 assemblies defined with one coolant channel for each of them in the previous step are coupled in a complete core. The results are compared with the previous step.

The principle of the second sub step is to limit the size of the numerical problem. The fact to consider the exact number of coolant channels is still acceptable with only one assembly, but the simulation would be numerically too heavy when it comes to the complete core. Thus, the second sub step checks that the results are almost the same with all the coolant channels or with an equivalent single coolant channel per assembly, and this new model is then used to complete the core simulation.

3.1 Equations and modeling tools

In the following steps, the fuel channels provide heat into the assembly. The heat equation is the following:

$$\rho c \frac{\partial T}{\partial t} = div(k * grad(T)) + q$$

where c is the specific heat, k the thermal conductivity and q the volumetric heat sources. This equation can be solved using the MOOSE Heat conduction Module (open-source).

3.2 Single assembly with 18 coolant channels

3.2.1 Simulation

An assembly is built using the geometrical parameters given in Table 8 and in Figure 2a. The coolant channels are defined in the Heat conduction input file as cylindrical holes in the assembly, and their external surfaces are defined as a special boundary of the fuel assembly.

A radial variation of the power density is imposed to the fuel channels. Four rings of fuel channels are defined, as shown in Figure 7. The difference of power density is also given in this figure.

In order to be as close as possible to a real assembly case, a length variation of the power density is also imposed in each fuel channel. The power density grows from the channel inlet where it measures 0.5 of its average value to a maximum in the middle. The power density then decreases and reaches the same value at the fuel channel outlet than at its inlet. A sinusoidal function is used to compute this power density variation.

All these power density variations are computed in order to have a total power exchange from the assembly equal to the 15 MWth provided by the core divided by the number of assemblies.

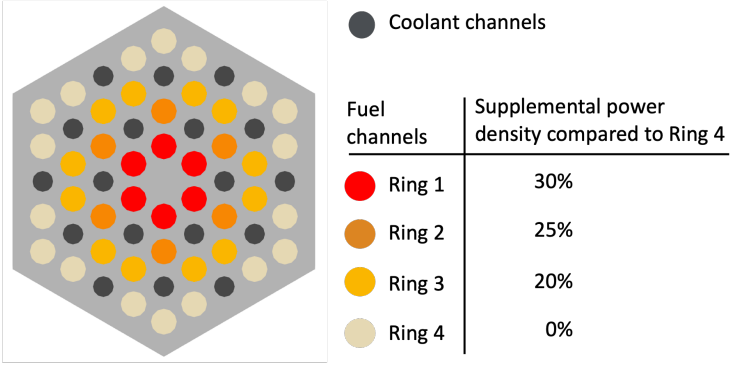

Figure 7: assembly pattern - definition of the fuel channels rings

Each coolant channel is modeled using the Thermal hydraulic Module and then connected to the Heat conduction model on the corresponding coolant channel boundary defined in the first paragraph. The Thermal hydraulic apps exchange information about the wall temperature (coming from the heat conduction model), the heat transfer coefficient and the fluid temperature (coming from the Thermal hydraulic sub apps). Using this way, the assembly transfers power to the coolant channels.

Boundary conditions are also imposed at the coolant channels inlet and outlet. They are deduced from the pressure, temperature and mass flow rate conditions obtained from the 1D previous simulation and adapted to each coolant channel.

Finally, some dependent temperature models are added for the fuel and graphite specific heats and thermal conductivities. The method is presented in the appendix.

3.2.2 Results

First and foremost, the power transferred by the fuel to the fluid must be verified. It is plotted in Figure8. The power fuel value is 0.271 MWth and is 55 times smaller than the total core power, because only one assembly among the 55 is considered in this simulation. An error appears between both steady state powers, provided from the fuel and received by the fluid. It is nevertheless consistent with the limit acceptable error because the gap is about 1%.

More precise measures of the temperatures in the assembly can be done with this simulation. They are represented in Figure 9a. The measured values are defined in a bit different way than in 2.3 because of the tools provided in this 3D-simulation. The fuel and moderator temperatures are provided instead of the wall temperature. An average is added, and the maximum and minimum temperatures are given in place of the inlet and outlet values.

The inlet and minimum ones must be equivalent. The power density reaches a minimum at the core inlet and the fluid temperature is cooler in this area. Nevertheless, the maximum and outlet temperatures could differ a bit, because of the sinusoidal power density definition. Consequently, the maximum temperatures should be reached between the middle of the assembly, where the power density is higher, and the outlet, because the fluid temperature is higher in the second half of the assembly than in the first one.

The moderator temperatures stay under 1340 K, which is smaller than what was measured in the 1D simulation for the wall temperature. This gap is in fact due to the more precise models on

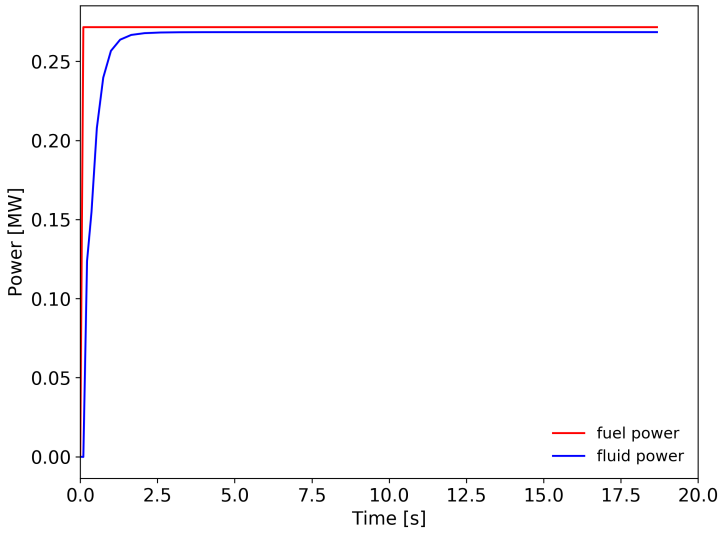

Figure 8: power transferred from the fuel and received by the fluid

the graphite specific heats and thermal conductivities. Their values at high temperature, which correspond to the steady state, are higher than the constant values that were provided in the 1D simulation. Consequently, the heat capacity of graphite is higher, and it transfers more easily its heat to the fluid.

The fuel temperature can be measured in this simulation. It stays under 1400 K, which is an acceptable limit.

A 3D representation of the temperature profile in the assembly is added in Figure 9b. It helps to visualize that the temperatures are smaller at the assembly inlet, higher as expected between the middle and the outlet and a bit lower around the coolant channels.

The fluid temperatures are plotted in Figure 10a, and the 3D profile is given in Figure 10b (the colors are put on the solid part of the assembly, but they correspond to the temperatures of the surrounded coolant channels). The minimum temperature, which is equivalent to the inlet temperature, is consistent with this one for the 1D simulation. The maximum fluid temperature, which should be really close to the outlet temperature as it appears in Figure 10b, is almost equal to the value measured in the 1D simulation, so 1190 K.

These minimum and maximum temperatures are in fact the average values of the minimum and maximum values among all the coolant channels. This method is used to be consistent with the results of the following simulation, where only one equivalent channel represents the 18 real coolant channels.

Finally, an average heat transfer coefficient is measured and plotted in Figure 11a, and a 3D representation of its values among all the coolant channels is provided in Figure 11b (once again, the colors are put on the solid part of the assembly, but they correspond to the heat transfer coefficient between the solid part and the surrounded coolant channels).

These values are close to the average value which was measured for the steady state of the 1D simulation.

The measured mass flow rate and pressure bring no more information, because they were fixed as inlet or outlet conditions on the single assembly model.

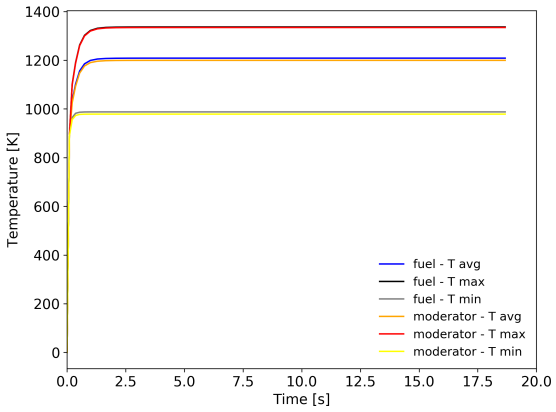

(a) plot of the temperatures in the assembly

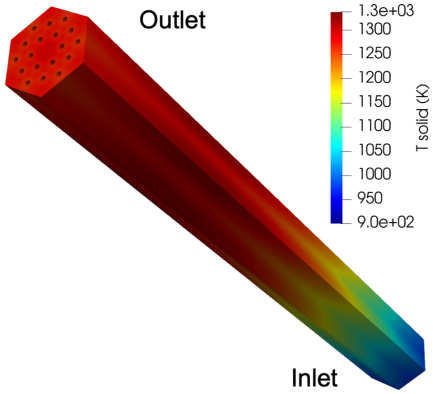

(b) 3D profile of the temperatures in the assembly

Figure 9: temperatures in the assembly

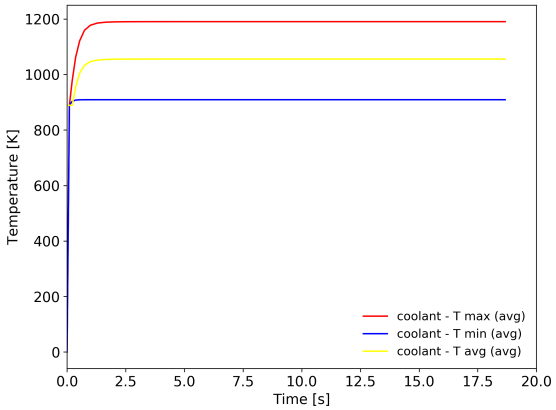

(a) plot of the temperature of the coolant

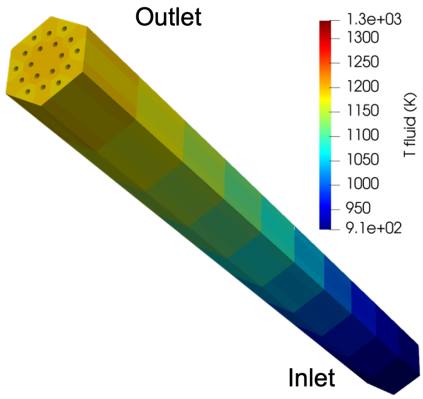

(b) 3D profile of the coolant temperature going through the assembly

Figure 10: coolant temperature

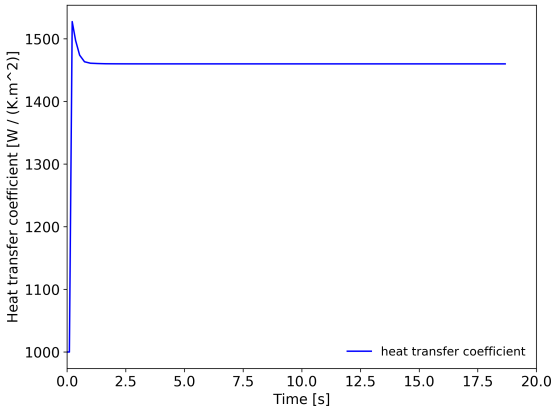

(a) plot of the average heat transfer coefficient

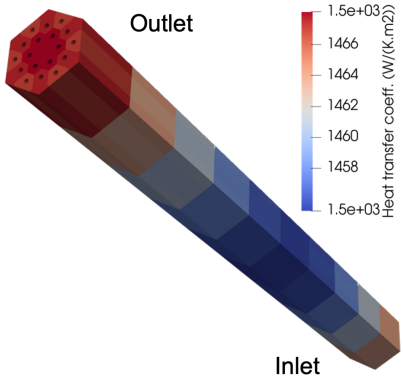

(b) 3D profile of the heat transfer coefficient at the coolant channels borders

Figure 11: heat transfer coefficient

3.3 Single assembly with one global coolant channel

3.3.1 Simulation

The previous simulated assembly could be multiplied by the number of assemblies in the complete core, but the simulation would be a too heavy problem, with a total of 990 coolant channels. A simplification can be suggested: the 18 coolant channels per assembly are reduced to only one, which must induce almost the same phenomena.

To do so, a unique coolant channel is simulated with the following properties:

- It must conduct the same total mass flow rate than with 18 small coolant channels: the declared section of the coolant channel is the sum of those of the 18 real coolant channels.
- It must receive the same power transfer, which is proportional to the heating perimeter of each real coolant channel multiplied their number in the assembly. Consequently, the declared heating perimeter is the sum of those of the 18 coolant channels.
- It must undergo the same friction force: the hydraulic diameter is the same than for a real coolant channel.

The results of this simulation must be compared with those of the assembly with 18 coolant channels. If the results are consistent, it will allow to use the second simulation to build the full core.

3.3.2 Results

The goal of this step is to verify if the results with one equivalent coolant channel are comparable with the case of an assembly coupled with the exact number of coolant channels.

The results of both simulations are deeply consistent. The plots are not reported in this part, because they seem to be the same than those presented in the previous subsection. A more precise calculation of the gaps between the steady state measures is reported in Table 11 and proves that these simulations are quite equivalent.

Table 11: Comparison of the steady state values of the main parameters for both simulations of one assembly

Parameter	Type	18 channels	one channel	relative gap
Coolant temperature (K)	minimum	909.0910	909.0915	0.000055%
-	maximum	1190.395	1190.396	0.000086%
-	average	1055.555	1055.645	0.0085%
Fuel temperature (K)	minimum	987.7426	987.8580	0.012%
-	maximum	1336.633	1334.352	0.17%
-	average	1208.557	1208.518	0.0032%
Moderator temperature (K)	minimum	978.6598	978.8318	0.017%
-	maximum	1334.388	1332.103	0.17%
-	average	1199.542	1199.754	0.017%
Power (kWth)	from the fuel	271.6039	271.6039	0%
-	to the coolant	268.4656	268.4656	0%
Heat transfer coeff. $(W/(K.m^2)$	average	1459.979	1459.979	0%

3.4 Full core

3.4.1 Simulation

A full core simulation is built using the assembly connected to a unique flow channel equivalent to the 18 real coolant channels per assembly.

The pattern is the same than presented in Figure 2b. It is surrounded by a graphite outer shield. This step is done using the Mesh tools of MOOSE.

3.4.2 Results

Once again, the plots of the fuel, moderator and fluid temperatures and of the average heat transfer coefficient are deeply similar. Of course, the measured powers differ because the 55 assemblies of the core are now considered. They are plotted in Figure 12.

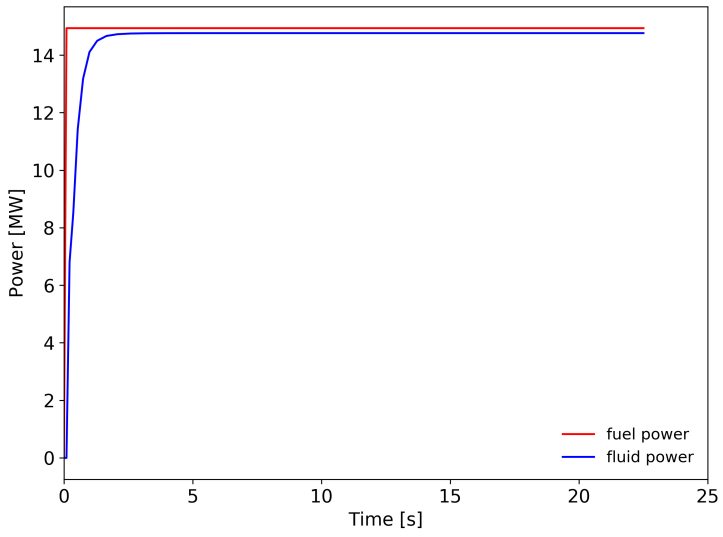

Figure 12: core - power transferred from the fuel and received by the fluid

Some 3D representations are nevertheless added in Figure 13. It makes visually appear the similarities between the full core and the single assembly simulations. In particular, one can remark that the heat transfer coefficient variation is really small: it seems to be almost constant in the whole core. It is consistent with the fact that with the 1D simulation, the core heat transfer coefficient was between 1463 and 1466 $W/(m^2.K)$.

As done previously, a comparison between the results of the single assembly with one equivalent coolant channel and the full core simulation is presented in Table 12. In this table, the power for one assembly is extrapolated to 55 assemblies to be able to compare it with the core values.

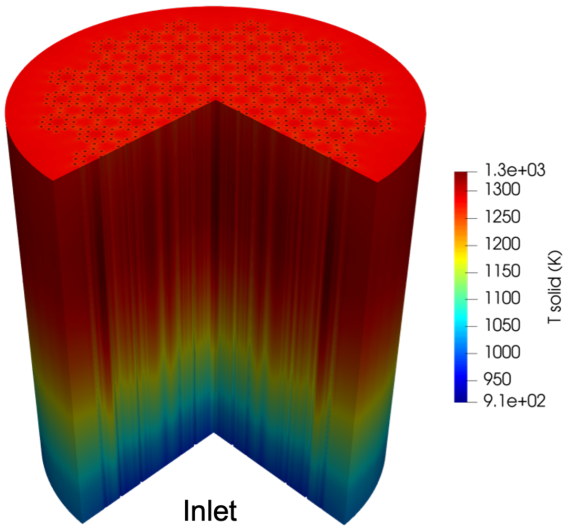

(a) temperature in the core

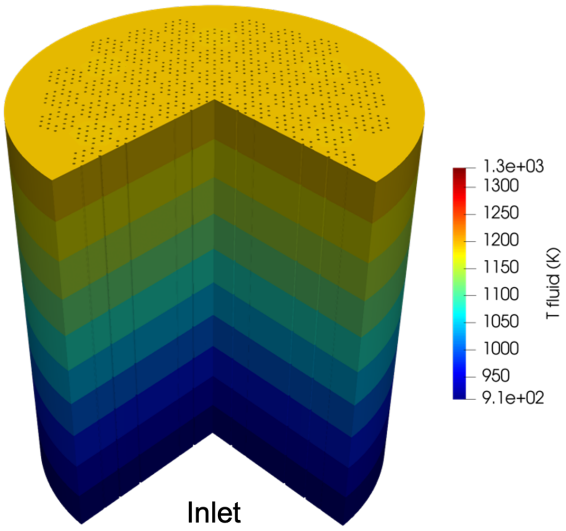

(b) coolant temperature

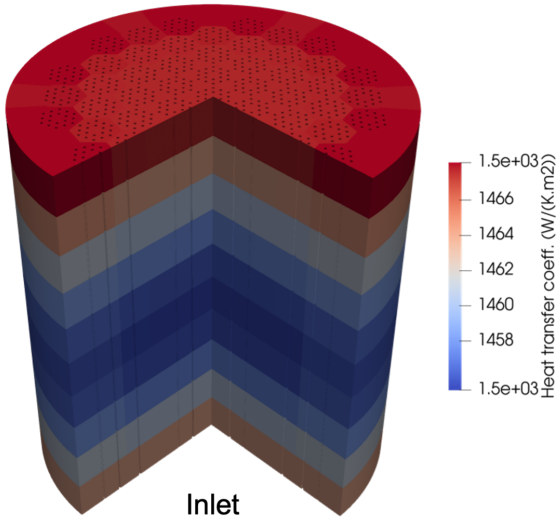

(c) heat transfer coefficient

Figure 13: temperatures in the core, in the fluid and heat transfer coefficient

Table 12: Comparison of the steady state values of the main parameters for the core simulation and the single simplified assembly

Parameter	Type	assembly	core	relative gap
Coolant temperature (K)	minimum	909.0915	909.0915	0%
-	maximum	1190.396	1190.401	0.00042%
-	average	1055.645	1055.849	0.019%
Fuel temperature (K)	minimum	987.8580	987.8582	0.000020%
-	maximum	1334.352	1334.359	0.0052%
-	average	1208.518	1208.376	0.012%
Moderator temperature (K)	minimum	978.8318	978.8320	0.000020%
-	maximum	1332.103	1332.109	0.00045%
-	average	1199.754	1199.614	0.012%
Power (MWth)	from the fuel	14.938215	14.93821	0.000030%
-	to the coolant	14.76561	14.76451	0.000014%
Heat transfer coeff. (W/(K.m^2))	average	1459.979	1460.244	0.018%

Conclusion

In this work, a relatively complete High Temperature Gas cooled Reactor simulation has been developed using the MOOSE tools. It illustrates the ability of this finite element framework to produce a realistic thermal hydraulic reactor model. The mechanical components of the one-dimensional simulation of the primary and secondary loops have been adapted to fit operating values. A simplification of the core has been built to get a complete helium circuit. This initial simulation of the two loops gives results in the line with those obtained for the three-dimensional model of the core. The latter makes it possible to verify the results consistency in a more precise model. This one provides material temperatures which are correct when compared to expectations. Consequently, most of the operating conditions computed and measured seem to be consistent with this type of high temperature reactor.

This study led to the publication of a brief summary of its conclusions for the American Nuclear Society (ANS) [11]. The input files developed during this internship and the results will be available on the INL Virtual Test Bed (VTB, open-source). It is a set of reactor simulations which are published online. Consequently, these models could be reused to be improved or complexified. Firstly, one could try to enhance the power efficiency of the developed reactor model, because the chosen operating value is lower than what is expected for HTGRs. Secondly, it is possible to imagine coupling these thermal hydraulic and heat conduction models with other physical phenomena.

Acknowledgments

I would like to thank everyone who helped me to do this internship and write my report.

First and foremost, I thank my mentor at Idaho National Laboratory, Dr. Lise C. Charlot, for her constant help during this internship. I would particularly like to thank her for her advises in defining the studied problem, the steps of reasoning and her assistance on how to use the simulation tools.

My thanks also go to Pr. François Willaime, who advised me during my internship search and suggested me to contact Idaho National Laboratory. His help gave me the opportunity to work in a particularly stimulating research environment.

I would like to thank Pr. Antoine Gerschenfeld for his thermal hydraulics applied to nuclear energy lessons at Ecole polytechnique which gave me the desire to go deeper in this subject. His courses were also a great help to do the study presented in this report.

I thank Pr. Christophe Josserand, who is the teacher supervising the internships in the field of mechanics applied to energy, for his guidance.

Ultimately, my thanks go to the staffs of the Ecole polytechnique and Idaho National Laboratory internship departments for taking care of all administrative matters.

This research made use of the resources of the High Performance Computing Center at Idaho National Laboratory, which is supported by the Office of Nuclear Energy of the U.S. Department of Energy and the Nuclear Science User Facilities under contract no. DE-AC07-05ID14517.

REFERENCES

[1] E. M. Duchnowski, R. F. Kile, K. Bott, L. L. Snead, J. R. Trelewicz, and N. R. Brown, "Pre-conceptual high temperature gas-cooled microreactor design utilizing two-phase composite moderators. part i: Microreactor design and reactor performance," *Progress in Nuclear Energy*, vol. 149, p. 104257, 2022.

[2] D. E. Shropshire, "Lessons learned from gen i carbon dioxide cooled reactors," Tech. Rep. INEEL/CON-04-01526, Idaho National Engineering and Environmental Laboratory, 04 2004.

[3] D. Copinger and D. Moses, "Fort saint vrain gas cooled reactor operational experience," Tech. Rep. NUREG/CR-6839; ORNL/TM-2003/223, Oak Ridge National Laboratory, 1 2004.

[4] C. Lu and N. R. Brown, "Fully ceramic microencapsulated fuel in prismatic high-temperature gas-cooled reactors: Design basis accidents and fuel cycle cost," *Nuclear Engineering and Design*, vol. 347, p. 108, 2019.

[5] E. M. Duchnowski, R. F. Kile, K. Bott, L. L. Snead, J. R. Trelewicz, and N. R. Brown, "Reactor performance and safety characteristics of two-phase composite moderator concepts for modular high temperature gas cooled reactors," *Nuclear Engineering and Design*, vol. 368, p. 110824, 2020.

[6] D. L. Mose, "Very High-Temperature Reactor (VHTR) Proliferation Resistance and Physical Protection (PR&PP)," Tech. Rep. ORNL/TM-2010/163, Oak Ridge National Laboratory, 8 2010.

[7] "GEN IV International Forum, Very-High-Temperature Reactor (VHTR)." `https://www.gen-4.org/gif/jcms/c_42153/very-high-temperature-reactor-vhtr`. (accessed: 01.07.2023).

[8] J. W. Sterbentz, P. D. Bayless, L. O. Nelson, H. D. Gougar, J. C. Kinsey, G. Strydom, and A. Kumar, "High-temperature gas-cooled test reactor point design," Tech. Rep. INL/EXT-16-38296, Idaho National Laboratory, 4 2016.

[9] "MOOSE framework, Recuperated Brayton cycle (resource page)." `https://mooseframework.inl.gov/modules/thermal_hydraulics/modeling_guide/recuperated_brayton_cycle/recuperated_brayton_cycle.html`. (accessed: 10.05.2023).

[10] D. P. Guillen and D. S. Wendt, "Integration of a microturbine power conversion unit in MAGNET," Tech. Rep. INL/EXT-20-57712, Idaho National Laboratory, 8 2020.

[11] S. M. de Boisset, L. C. Charlot, T. Freyman, and J. Hansel, "Modeling a gas-cooled microreactor balance of plant for the virtual test bed," in *Submitted to ANS winter meeting, October 2023*, 2023.

[12] "MOOSE framework GraphiteMatrixThermal (resource page)." `https://mooseframework.inl.gov/bison/source/materials/GraphiteMatrixThermal.html`.

A Material Properties

This appendix details the method applied to get temperature-dependent models of the thermal conductivities and specific heats of the core solid materials. One the other hand, thermodynamic fluid properties are already determined using the Thermal hydraulic Module tools. The calculations in this appendix are done using information from open-source MOOSE resources [12].

Graphite properties

Specific heat

The moderator used in the assembly is H-451 graphite [1]. The MOOSE resources [12] provide the Butland and Madison specific heat model. It can be applied to temperatures between 250 K and 3000 K. Consequently, the values can be considered in the temperature range of this study.

The proposed model is the following, and is plotted in Figure 14a:

$$c_p = 4184(0.54212 - 2.42667 * 10^{-6} * T - \frac{90.2725}{T} \frac{43449.3}{T^2} + \frac{1.59309*10^7}{T^3} - \frac{1.43688*10^9}{T^4})$$

Thermal conductivity

A model of the thermal conductivity of H-451 graphite is provided in the MOOSE resources [12]. It is also a fluence dependent model, where fluence is the integrated neutronic flux over the time. Neutronic phenomena are nevertheless not considered in this study.

Typical neutronic flux are between 10^{10} and $10^{12} neutrons.m^{-2}.s^{-1}$. The lattice pitch and packing fraction choices lead to a cycle length of approximately 2 Effective Full Power Years (EFPY) [1]. Consequently, the fluence increases from 0 at the beginning to $3.10^{17} neutrons.m^{-2}$ at the maximum. Figure 14b does not present a deep variation between the models for a fluence equal to 0 or to $2.10^{24} neutrons.m^{-2}$. The maximum fluence previously computed is moreover relatively close to 0 $neutrons.m^{-2}$. Consequently, the model on k is considered independent from the neutronic fluence.

Fuel properties

Specific heat

The fuel material is a mix of TRISO particles, whose packing fraction is 50%, in a H-451 graphite matrix. Homogenized models are provided in [12]. The specific heat of the fuel is computed using the following formula, where PF is the packing fraction:

$$c_p = PF * c_p(TRISOparticle) + (1 - PF) * c_p(graphite)$$

In order to compute this value, the TRISO particle specific heat needs also to be known. [12] provides a homogenized value for this parameter, calculated using the specific heats of each layer:

$$c_p(TRISOparticle) = 748.72 J/(kg.K)$$

The temperature dependence of the fuel specific heat is plotted in Figure 15a.

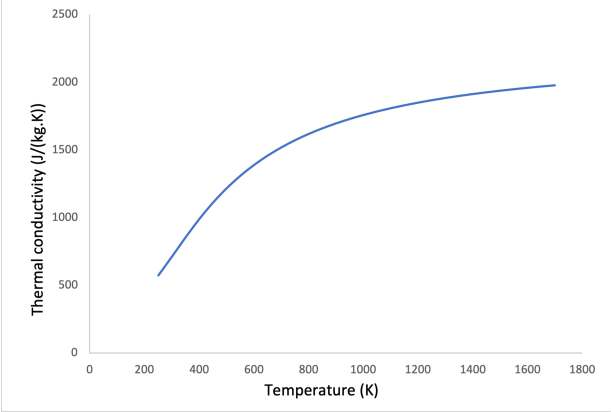

(a) H-451 graphite - specific heat

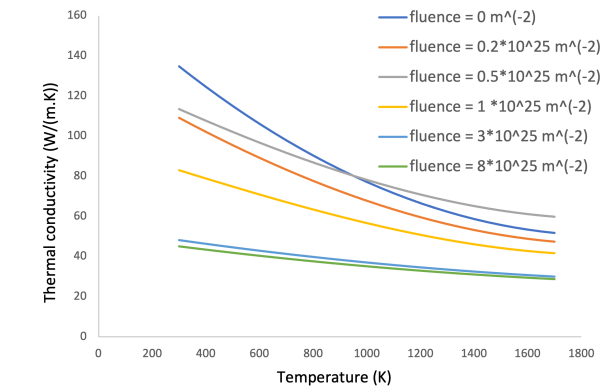

(b) H-451 graphite - thermal conductivity

Figure 14: graphite properties

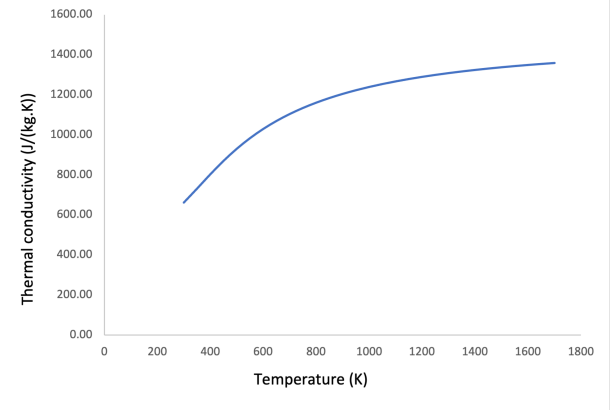

(a) fuel - specific heat

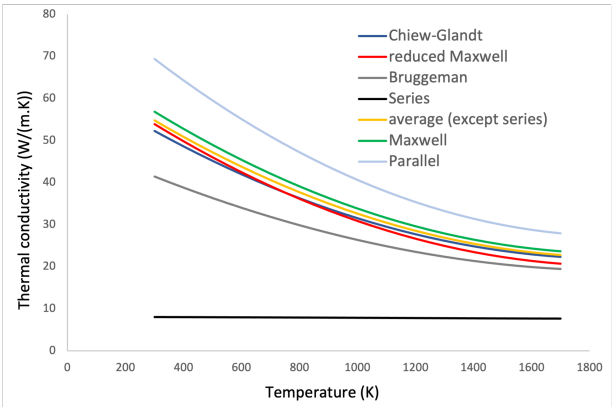

(b) fuel - thermal conductivity

Figure 15: graphite properties

Thermal conductivity

The calculation of the homogenized fuel thermal conductivity is more complex. [12] provides several models, developed by McLaughlin, Chiew and Glandt, Maxwell and Bruggeman, a harmonic mean (series) model and a volume average (parallel) model. Each of them depends on the packing fraction, the thermal conductivity of the H-451 graphite but also on the thermal conductivity of the homogenized TRISO particles. A constant value for this parameter is provided in [12]:

$k_{TRISO} = 4.13 W/(m.K)$

The several models are plotted in Figure 15b. The series model seems to be not consistent with the others, while the average of the five other models is close to the Chiew-Glandt, Maxwell and reduced Maxwell models. The Chiew-Glandt model is consequently chosen as a representative model for the fuel behavior.